GeroScience (2024) 46:1107–1127
https://doi.org/10.1007/s11357-023-00863-w

ORIGINAL ARTICLE

SIRT1 safeguards adipogenic differentiation by orchestrating anti-oxidative responses and suppressing cellular senescence

An Yu · Ruofan Yu · Haiying Liu · Chenliang Ge · Weiwei Dang

Received: 24 August 2022 / Accepted: 23 June 2023 / Published online: 8 July 2023

Abstract Adipose tissue is an important endocrine organ that regulates metabolism, immune response and aging in mammals. Healthy adipocytes promote tissue homeostasis and longevity. SIRT1, a conserved NAD^+-dependent deacetylase, negatively regulates adipogenic differentiation by deacetylating and inhibiting PPAR-γ. However, knocking out SIRT1 in mesenchymal stem cells (MSCs) in mice not only causes defects in osteogenesis, but also results in the loss of adipose tissues, suggesting that SIRT1 is also important for adipogenic differentiation.

Here, we report that severe impairment of SIRT1 function in MSCs caused significant defects and cellular senescence during adipogenic differentiation. These were observed only when inhibiting SIRT1 during adipogenesis, not when SIRT1 inhibition was imposed before or after adipogenic differentiation. Cells generate high levels of reactive oxygen species (ROS) during adipogenic differentiation. Inhibiting SIRT1 during differentiation resulted in impaired oxidative stress response. Increased oxidative stress with H_2O_2 or SOD2 knockdown phenocopied SIRT1 inhibition. Consistent with these observations, we found increased p16 levels and senescence associated β-galactosidase activities in the inguinal adipose tissue of MSC-specific SIRT1 knockout mice. Furthermore, previously identified SIRT1 targets involved in oxidative stress response, FOXO3 and SUV39H1 were both required for healthy adipocyte formation during differentiation. Finally, senescent adipocytes produced by SIRT1 inhibition showed decreased Akt phosphorylation in response to insulin, a lack of response to adipocytes browning signals, and increased survival for cancer cells under chemotherapy drug treatments. These findings suggest a novel safeguard function for SIRT1 in regulating MSC adipogenic differentiation, distinct from its roles in suppressing adipogenic differentiation.

Keywords Adipogenesis · Differentiation · MSC · Oxidative stress · Senescence · SIRT1

Supplementary Information The online version contains supplementary material available at https://doi.org/10.1007/s11357-023-00863-w.

A. Yu · C. Ge
Yunnan Key Laboratory for Basic Research On Bone and Joint Diseases &, Yunnan Stem Cell Translational Research Center, Kunming University, Kunming 650214, Yunnan, China

A. Yu · R. Yu · H. Liu · W. Dang (✉)
Baylor College of Medicine, Huffington Center On Aging, 1 Baylor Plaza, Houston, TX 77030, USA
e-mail: weiwei.dang@bcm.edu

Introduction

Adipocytes are the primary cell type of the adipose tissue and healthy adipocytes are essential for maintaining homeostasis [1] and longevity[2]. Patients with the adipose tissue disorders of obesity or

lipodystrophy have dysfunctional adipocytes, characterized by increased expression of inflammatory factors, increased insulin resistance and decreased secretion of adiponectin [3–6]. Recently, it has been suggested that adipocyte senescence may be a cause of dysfunction and increased inflammation in the adipose tissue [7]. In a mouse model with the *XP-V* gene knockout, senescent adipocytes are causatively linked to the development of systemic metabolic abnormalities including hepatic steatosis, hyperleptinemia, hyperinsulinemia and glucose intolerance [8]. Senescence is a state of cell cycle arrest, a common cellular response to certain intrinsic and/or extrinsic insults or stresses. Along with the cessation of proliferation, senescent cells show several other hallmarks. These hallmarks include: high levels of expression for cyclin-dependent kinase inhibitors, such as p21 and p16, increased senescence associated β-galactosidase activities, as well as senescence-associated secretory phenotype (SASP), a phenomenon of increased secretion of pro-inflammation cytokines, chemokines, growth factors and proteases [9]. Clearance of senescent cells by either genetic [10] or pharmacological [11] approaches can slow down the aging process and extend the lifespan in mice. Previously the field maintained that post-mitotic cells did not undergo senescence in response to stress [12]. However, emerging evidence suggests that terminally differentiated post-mitotic cells including neurons [13, 14] and adipocytes [8, 15] can possess hallmarks of senescence.

SIRT1, an NAD^+-dependent protein deacetylase, is one of the seven different sirtuins in mammals. It has broad substrates that include histones, as well as many important regulators of various cellular processes, such as FOXO3 [16], p53 [17], and p65 [18]. SIRT1 has been shown to function as a negative regulator of adipogenic differentiation in both 3T3-L1 adipocytes [19] and in multipotent mesenchymal stem cells [20]. This inhibitory effect of SIRT1 on adipogenic differentiation has been further confirmed in vivo using the $SIRT1^{\pm}$ mouse model [21]. Nevertheless, mice with MSC-specific SIRT1 knockout show a 35% reduction of subcutaneous fat with smaller adipocytes, a phenotype exasperated with age, when the fat reduction extends to 64% [22]. In human bone marrow-derived MSCs, SIRT1 knockdown results in decreased adipogenic differentiation efficiency indicated by decreased lipid droplet accumulation [23]. These lines of evidence suggest that SIRT1 may also play a supporting role in adipogenic differentiation in MSCs. Furthermore, MSC-specific SIRT1 knockout mice show signs of metabolic syndrome as indicated by increased blood triglyceride and glucose levels [22]. Therefore, the roles of SIRT1 in MSCs and their derived adipocytes are more complicated than previously thought.

Here we investigated SIRT1's function in supporting adipogenic differentiation in MSCs. We found that severe impairment of SIRT1 in MSCs during differentiation leads to dramatic defects: reduced lipid accumulation, decreased adiponectin, elevated pro-inflammatory cytokines and increased cellular senescence. These defects were not observed when SIRT1 was inhibited before or after adipogenic differentiation, suggesting a specific function for SIRT1 during the differentiation process. During adipogenic differentiation, cells experience high levels of oxidative stress. We found that inhibiting SIRT1 greatly compromised key oxidative stress response pathways. Treating differentiating cells with H_2O_2 or knocking down SOD2 phenocopied SIRT1 inhibition, suggesting that differentiation defects induced by SIRT1 inhibition were due to increased oxidative stress. Consistent with these findings, we also observed increased p16 protein levels and senescence associated β-galactosidase activities in the inguinal adipose tissue of MSC-specific SIRT1 knockout mice. Furthermore, previously identified SIRT1 targets that are involved in oxidative stress response, FOXO3 and SUV39H1 were both required for healthy adipogenic differentiation. Finally, senescent adipocytes caused by SIRT1 inhibition during differentiation decreased Akt phosphorylation in response to insulin, diminished the browning capacity of adipocytes and promoted cancer cell survival under chemotherapy drug treatments. Our findings reconcile seemingly contradictory effects of SIRT1 on adipogenic differentiation and support a function of SIRT1 in activating oxidative stress response during differentiation to prevent adipocyte senescence.

Materials and methods

Reagents

All chemicals used and all shRNA clones were purchased from Sigma-Aldrich, the Cat# of all shRNA

clones were listed in Supplementary Table 2. DMEM medium and fetal bovine serum were purchased from Gibco. F12/DMEM medium was purchased from Hyclone. Antibodies of SIRT1 (ab12193), β-actin (ab8226), Histone H3 (ab1791), FOXO3 (ab70315), SUV39H1 (ab12405), p16 (ab211542) and adiponectin (ab22554) were purchased from Abcam. Antibodies of AKT (#4691), p-AKT (#4060), IL-6 (#12,912) and ATM (#2873) were purchased from Cell Signaling Technology. H3K9me3 antibody (39,241) was purchased from Active Motif. Acetyl-lysine antibody (06–933) was purchased from Millipore. The HRP-coupled secondary antibodies were purchased from Abcam (ab6728 and ab6721).

Animals

All mice were in a C57Bl/6 background. Mesenchymal stem cells specific SIRT1 knockout mice (MSCKO) were generated by crossing the SIRT1 allele containing a floxed exon 4 with Cre-expressing mice driven by the mesenchymal progenitor cell-specific Prrx1-cre promoter [22]. Both SIRT1 floxed exon 4 mice and Prrx1-cre mice were purchased from Jackson Laboratory. All mice were housed at 25 °C and 12:12 h light/dark cycle. All animal procedures were performed in accordance with NIH guidelines and with the approval of the Baylor College of Medicine Institutional Animal Care and Use Committee.

Cell culture and treatments

Mouse mesenchymal stem cells line C3H10T1/2, human primary umbilical cord mesenchymal stem cells (ucMSCs), and mouse liver cancer cells line Hepa1-6 were all purchased from ATCC (www.atcc.org). Human primary bone marrow mesenchymal stem cells (B-MSCs) were purchased from Extem Bioscience. Before adipogenic differentiation induction, C3H10T1/2 cells and human MSCs were all maintained in a hypoxia incubator (37 °C, 5% CO_2, 3% O_2); C3H10T1/2 cells were maintained in DMEM/F12 medium with 10% fetal bovine serum, both human uMSCs and B-MSCs were maintained in low glucose (1 g/L) DMEM medium with 10% fetal bovine serum. During adipogenic differentiation, C3H10T1/2 cells and human primary cells were maintained in a normal oxygen incubator (37 °C, 5% CO_2).

Home-made adipogenic induction medium was used for mouse C3H10T1/2 cells adipogenic differentiation, it is high glucose (4.5 g/L) DMEM medium that contains 10% fetal bovine serum, 0.5 mM isobutylmethylxanthine (IBMX), 2 µM dexamethasone (DEX), 10 µg/ml insulin and 2 µM rosiglitazone. Adipogenic induction medium for both human uMSCs and human B-MSCs differentiation was purchased from Gibco.

After differentiation, mature adipocytes were maintained in high glucose DMEM medium with 10% fetal bovine serum in a normal oxygen incubator (37 °C, 5% CO_2). Live and dead Hepa1-6 cells were counted by an automated cell counter (Countess Invitrogen).

During the adipogenic differentiation induction, H2O2 was added into the induction medium with final concentration of either 100 µM or 300 µM, and the control group is the adipogenic induction medium only (Fig. 4F).

48 h after 8-day adipogenic differentiation, C3H10T adipocytes were treated with 2.5 µM Berberine for 24 h to induce browning (Fig. 6C).

Generation of single cell derived SIRT1 knockout C3H10T1/2 clones by CRISPR/cas9

LentiCRISPR v2 vector can be inserted with guide RNA (gRNA) and used to generate Lentivirus to knockout genes in mammalian cells [24]. It has been shown that SIRT1 can be knocked out by using CRISPR/cas9 [25]. The LentiCRISPR v2 vector was obtained from addgene (Addgene: lentiCRISPR v2). Five single guide RNA (sgRNA) sequences were designed on the website: https://www.atum.bio/eCommerce/cas9/. The sequences of the five sgRNAs were listed in Supplementary Table 3. The sgRNA was ligated into the lentiCRISPR v2 vector, then all vectors were sent to be sequenced to verify the correct insertion. After sequencing, all vectors were compacted into a lentivirus, and the control is the lentivirus made by an intact lentiCRISPR v2 vector. Firstly, the knockout efficiencies of the five sgRNAs were tested, and the results showed that all five sgRNA are able to knockout SIRT1 to a certain degree, and the sgRNA4 has the highest knockout efficiency (Fig. S1A). Secondly, three sgRNAs were picked randomly, and they are sgRNA1, sgRNA4, and sgRNA5. The lentivirus of sgRNA1, sgRNA4, and

sgRNA5 were used to infect C3H10T1/2 cells then followed by three days of puromycin selection, and the western blot result showed that they are indeed efficient sgRNA (Fig. S1B and Fig. S9H). Notably, at this stage the cells of each sgRNA are in the pooled form, therefore SIRT1 can not be completely knocked out (Fig. S1B). Thirdly, single cells of each sgRNA virus infected cells were isolated into 96 well plates, only one cell was put into one well to produce single cell derived cell clones. After several rounds of western blotting selection, SIRT1 knockout clones produced by each sgRNA were obtained (Fig. S1C and Fig. S9I). The control cells are also single cell derived clone by using lentivirus made from intact lentiCRISPR v2 vector without gRNA insertion.

Quantitative real time PCR (Q-PCR) and western blots

Total RNA was isolated by QIAzol Lysis Reagent (QIAGEN). The reverse transcriptase and Fast SYBR Green Master Mix are from Thermo Fisher Scientific applied biosystem. For each sample, 2 μg total RNA was used to perform reverse transcription. Q-PCR was carried out in a total volume of 12 μl with SYBR Green Master mix on a ViiA7 thermal cycler (Life Technologies). For samples from C3H10T1/2 cells and Hepa1-6 cells, mouse 36B4 (ribosomal protein, large, P0; Rplp0) was used as the internal reference and amplified in parallel. For samples from human primary mesenchymal stem cells or differentiated adipocytes, human β-actin was used as the internal reference. The PCR conditions were 95 °C for 3 min, followed by 40 cycles of 95 °C for 15 s, 60 °C for 15 s, and 72 °C for 15 s. Cycles threshold values normalized to that of the internal reference, and the relative gene expression levels were calculated by the $2^{-\Delta\Delta Ct}$ method. All Q-PCR primers sequence and serial numbers of all shRNA clones were indicated in Supplementary Tables 1 and 2.

Western blot experiments were carried out as previously described [26]. All human cells, mouse cells, and mouse inguinal adipose tissue were lysed in a buffer containing 50 mM Tris/HCl (pH 7.4), 150 mM NaCl, 1% NP40 (v/v), 0.25% sodium-deoxycholate, 1 mM sodium orthovanadate,1 mM sodium fluoride, 1 mM EGTA, 10 μg/mL leupeptin and 20 μg/mL aprotinin. Inguinal adipose tissue was homogenized with the lysis buffer. After incubation for 1 h at 4 ℃, the suspension was centrifuged at 10,000 g for 5 min and the pellets were discarded. Protein aliquots from each sample were separated by SDS-PAGE then all proteins were transferred onto polyvinylidene difluoride membranes. The membranes were blocked with TBST buffer (20 mM Tris–HCl, 137 mM NaCl, and 0.05% Tween-20) containing 2% BSA at room temperature for 60 min then incubated overnight with a 1:1000 dilution of appropriate primary antibodies. After extensive washing, the membranes were incubated with horseradish peroxidase-conjugated secondary antibodies (1:10,000) for 1 h at room temperature and visualized using a clarity western ECL substrate (BIO-RAD). All western blot quantification results that are not shown in the main figures can be found in Supplementary Figs. 8–10.

DHE staining and adipocytes conditioned medium collection

DHE staining experiments were carried out as previously described [27] with slight modifications: cells were washed with PBS for 5 min, then were incubated with 50 μM DHE (Dihydroethidium) for 30 min in a dark 37 ℃ incubator. Then cells were washed with PBS for 10 min. Conditioned media were collected as a method reported before [28] with a slight modification: adipocytes were incubated with high glucose (4.5 g/L) DMEM medium with 5% fetal bovine serum for 48 h, then the conditioned medium was collected and stored at -20 ℃.

Senescence-associated β-galactosidase (SA-β-Gal) activity, co-immunoprecipitation, and immunohistochemistry staining

SA-β-Gal staining kit was purchased from Cell Signaling Technology. Cells and mouse inguinal adipose tissue were washed in PBS, fixed for 15 min (room temperature) in 2% formaldehyde and 0.2% glutaraldehyde, washed, and incubated at 37 ℃ with a fresh staining solution for 12 h. The SIRT1 co-immunoprecipitation and FOXO3 immunostaining were carried out according to the methods that were previously described [26]. Briefly, each protein sample (700 μg) was incubated with 2 μg SIRT1 or Foxo3 antibody for 12 h on a rotator at 4℃, then 50 μl protein G coupled magnetic beads were added into each sample for 4 h additional rotating incubation. Samples were washed

five times in PBS, each time 10 min, then magnetic beads were collected. For immunostaining: cells were fixed for 30 min in 4% formaldehyde at room temperature, then cells were permeated by 0.5% Triton X-100 for 15 min, after that cells were blocked by 2% BSA. Cells were incubated with Foxo3 antibody (1:100) for 12 h at 4 ℃, after washing, cells were incubated with fluorescence coupled secondary antibody (1:400) for 12 h at 4 ℃. Cells were washed for 3 times and kept at 4 ℃.

Oil red O quantification, cell SA-β-gal quantification and adipose tissue SA-β-gal intensity measurement

Oil red o staining quantification is based on a previous study [29] with modification:

Specifically, the figure is imported, and total cell areas (as an indication of cell number) are manually circled out using the freehand tool. Stained regions are selected by the threshold tool, then performed reciprocal calculation and measured (since the default measurement of imageJ is greyscale, the darker region will have a lower value, hence reciprocal is needed). Inden is used as the total intensity of the selected area. The final relative density is calculated by Inden/cell area. The whole field of three images of each experimental group was used to quantify oil red O content.

For cellular SA-β-gal positive ratio: in each experimental group, three images were used. Total cell number and SA-β-gal positive cell number were counted, and the SA-β-gal positive ratio is calculated by SA-β-gal positive cell number/total cell number.

Adipose tissue SA-β-gal intensity measurement was performed by a similar method: Stained tissues are selected by the threshold tool, then performed reciprocal calculation and measured (since the default measurement of image J is greyscale, the darker region will have a lower value, hence reciprocal is needed). Inden is used as the total intensity of the selected area. The final relative density is calculated by Inden/tissue area.

Other fluorescent figure quantification

Similar to the method to quantify Oil Red O [29]. Total intensity is measured without normalization with threshold tools. Inden is used as an indication of intensity.

Statistical analysis

All Q-PCR experiments and Hepa1-6 cells chemoresistance experiments were repeated at least three times with similar results. Data are presented as means ± SD. Student's t test was used for statistical comparison. The one-way ANOVA test was used for multi-group statistical comparison. $P < 0.05$ was considered statistically significant.

Results

Expression levels-dependent effects of SIRT1 on MSC adipogenic differentiation

SIRT1 has been considered a suppressor for adipogenic differentiation [19–21]. However, MSC-specific SIRT1 knockout mice exhibit significantly reduced levels of subcutaneous fat and smaller adipocytes than controls [22], suggesting that SIRT1 may also play a role in supporting adipogenesis. We hypothesize that the roles of SIRT1 on adipogenic differentiation may be expression levels-dependent. To test this, we used shRNA clones with different knockdown efficiencies, prepared lentiviruses and transfected the mouse C3H10T1/2 MSCs (Fig. 1A, and Fig. S9A). Indeed, whereas a moderate reduction in SIRT1 expression resulted in an increase in lipid droplets, a severe knockdown of SIRT1 caused decreased lipid droplet accumulation (Fig. 1B-C). Interestingly, the severe SIRT1 knockdown increased cellular senescence as shown by the significantly increased senescence associated with β-galactosidase (SA-β-Gal) activities (Fig. 1B-C). This change was not obvious in cells treated with moderate SIRT1 knockdown. As expected, the expression of p16, a cyclin-dependent kinase inhibitor (CKI) and a critical senescence marker, was activated in cells with the severe SIRT1 knockdown (Fig. 1D-E and S2A). The expression levels of SIRT1 and p16 during adipogenic differentiation were shown in Supplementary Fig. 2A and 9 J (Fig. S2A and S9J). To confirm that severe loss of SIRT1 function caused adipogenic defects and increased senescence, SIRT1 knockout C3H10T1/2 clones were generated by CRISPR/cas9 with three different single guide RNA (sgRNA) (Fig. S1C). Upon adipogenic differentiation, all three SIRT1 knockout cell clones displayed dramatically decreased

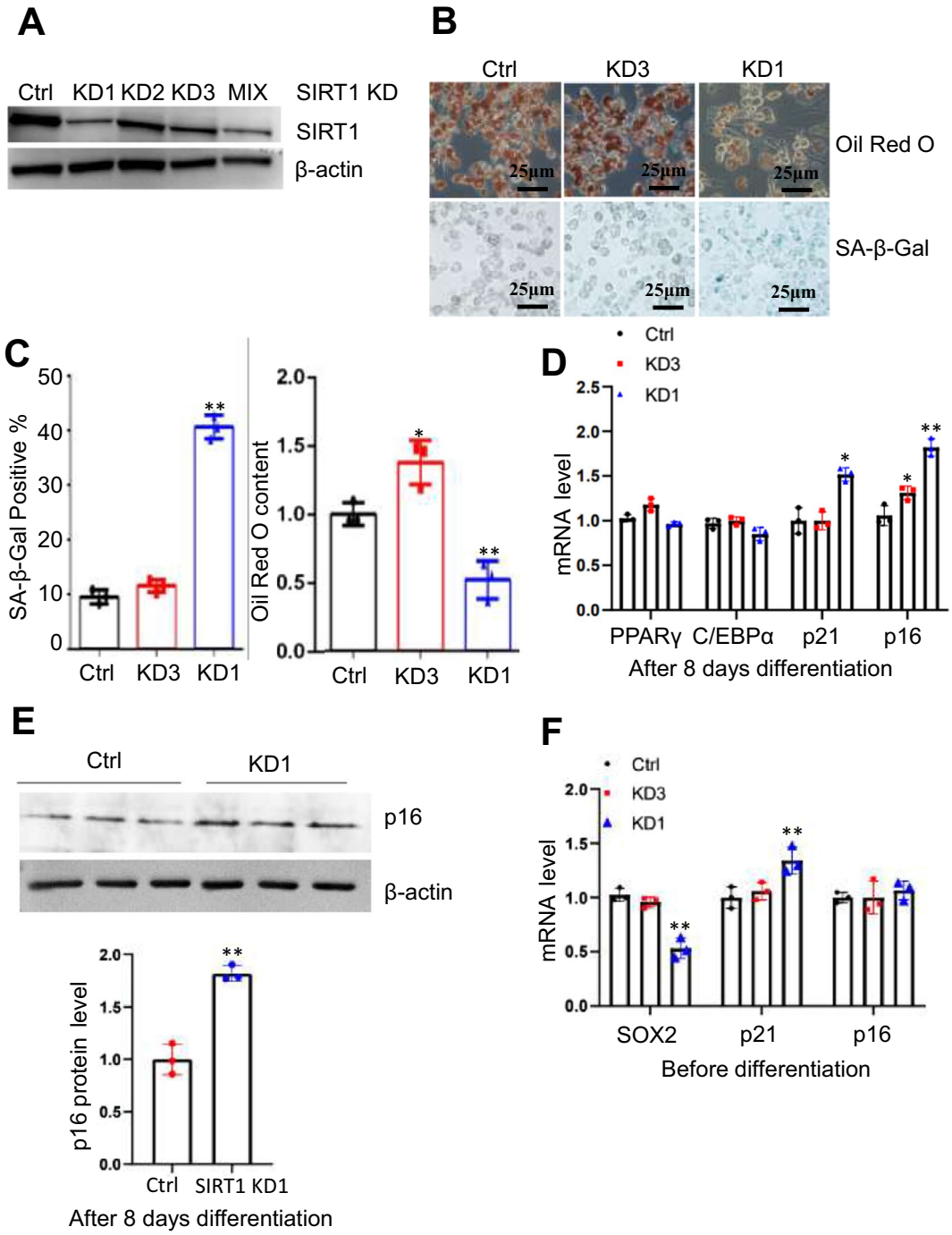

lipid droplet accumulation (Fig. S1D) and significantly increased p16 and IL-6 expression (Fig. S1E). These results are highly consistent with the severe SIRT1 knockdown results (Fig. 1B-E), indicating that only severe loss of SIRT1 function causes adipogenic defects. Interestingly, the expression of adipogenic differentiation master regulators PPARγ and C/EBPα were not significantly affected by severe SIRT1 knockdown (Fig. 1D), suggesting that the adipogenic differentiation program was still activated as expected. As a control, knocking down SIRT1 in undifferentiated MSCs did not elevate the expression

◂**Fig. 1** Severe SIRT1 knockdown increased cellular senescence during adipogenic differentiation in C3H10T1/2 mesenchymal stem cells. (Ctrl: control, KD: knockdown, SA-β-Gal: senescence associated β galactosidase, One-Way ANOVA test was used for multi-group statistical comparison.) (**A**) Cell strains with different SIRT1 protein dosages were produced by lentivirus mediated SIRT1 knockdown, and different shRNA clones with different knockdown efficiency were identified by western blotting. Proteins from different cell strains were extracted on day 8 after 3 days of puromycin selection. (**B**-**C**) Severe SIRT1 knockdown (SIRT1 KD 1) decreased lipid droplets accumulation and increased SA-β-Gal activity after 8 days of adipogenic differentiation compared to control shRNA cells, (**B**-**C**) while moderate SIRT1 knockdown (SIRT1 KD 3) increased lipid droplets accumulation and did not increase SA-β-Gal activity. (**D**) After 8 days of adipogenic differentiation, severe SIRT1 knockdown (SIRT1 KD1) significantly increased p21 and p16 mRNA levels, while moderate SIRT1 knockdown (SIRT1 KD3) only slightly increased p16 mRNA (Data represent mean ± SD, $n = 3$, $^{*}p < 0.05$, $^{**}p < 0.01$). (**E**) After 8 days of adipogenic differentiation, severe SIRT1 knockdown increased the p16 protein level. (**F**) In undifferentiated cells, neither moderate (KD3) nor severe (SIRT1 KD1) SIRT1 knockdown increased p16 mRNA level, while only severe SIRT1 knockdown decreased sox2 and increased p21 mRNA expression (Data represent mean ± SD, $n = 3$, $^{*}p < 0.05$, $^{**}p < 0.01$)

of p16 (Fig. 1F). Rather, the expression of p21, another cyclin-dependent kinase inhibitor associated with cell cycle arrest and apoptosis inhibition, was activated. Further, reduced expression of SOX2 indicates impaired stem cell functions, consistent with a previous report [23]. The differences in CKI expression induced by the severe SIRT1 knockdown during differentiation vs prior to differentiation suggest a distinct function of SIRT1 during adipogenic differentiation from its functions in stem cell maintenance.

Severe defects in adipogenesis when SIRT1 was inhibited during differentiation

Since SIRT1 appeared to have a novel function to support adipogenic differentiation besides its roles in maintaining stem cell functions, we then focus on the differentiation process. To dissect at which stage of adipogenic differentiation SIRT1 plays the supportive role, we designed an experiment to compare the MSC differentiation outcomes when SIRT1 activities were inhibited by a specific inhibitor, EX-527, only during either the eight days before differentiation, or during the eight days of differentiation, or during the eight days after differentiation (Fig. 2A). A relatively high concentration (60 μM) of EX-527 was used to achieve a level of inhibition for SIRT1 like severe knockdown or knockout. We found that, only during adipogenic differentiation, SIRT1 inhibition caused a drastic decrease in lipid droplet accumulation and a significant increase in the senescence marker SA-β-Gal staining, whereas no adverse effects on differentiation can be observed for cells treated with the inhibitor before differentiation (Fig. 2B-E and S2C-D). EX-527 treatment after differentiation may negatively affect mature adipocytes by decreasing adiponectin expression (Fig. 2G) but did not increase cellular senescence as the treatment during differentiation did (Fig. 2B-C). There is a decrease of p21 mRNA expression in undifferentiated cells treated with EX-527 (Fig. 2D), whereas p21 mRNA level was increased in undifferentiated cells by SIRT1 knockdown (Fig. 1F) indicating EX-527 may have side effects in undifferentiated cells. Resistin is a typical pro-inflammatory adipokine that induces insulin resistance in mice. 8 days of EX-527 treatment before adipogenic differentiation did not affect lipid accumulation (Fig. 2B), cellular senescence (Fig. 2C), and pro-inflammatory adipokine TNF-α (Fig. 2E); however, resistin was significantly up-regulated (Fig. 2E) indicating a higher inflammation status and that 8 days EX-527 treatment before differentiation indeed slightly affect the cells. Consistent with the adipogenesis and senescence phenotypes, MSCs treated with EX-527 during differentiation showed dramatic changes in transcription: reduced expression of adipogenic genes PPARγ, C/EBPα, and adiponectin (Fig. 2F and S2B and S10A); and increased expression of p16 and SASP factors, such as IL-6 and TNF-α (Fig. 2F). These phenotypic and gene expression changes suggest that the lack of SIRT1 activity during adipogenesis results in dysfunctional adipocytes. Little or only slight changes in these genes were observed for MSCs with treated with EX-527 before differentiation (Fig. 2D-G). As a control, inhibiting SIRT1 in undifferentiated MSCs was not sufficient to cause cellular senescence, monitored by both the SA-β-Gal activities (Fig. S3A) and p16 expression (Fig. 2D), consistent with the observation made in undifferentiated MSCs with SIRT1 knockdown (Fig. 1D). It should also be noted that p21, but not p16, was down-regulated in EX-527 treated undifferentiated cells (Fig. 2D), consistent with the idea that SIRT1 play distinct functions between proliferating stem cells and differentiating stem cells.

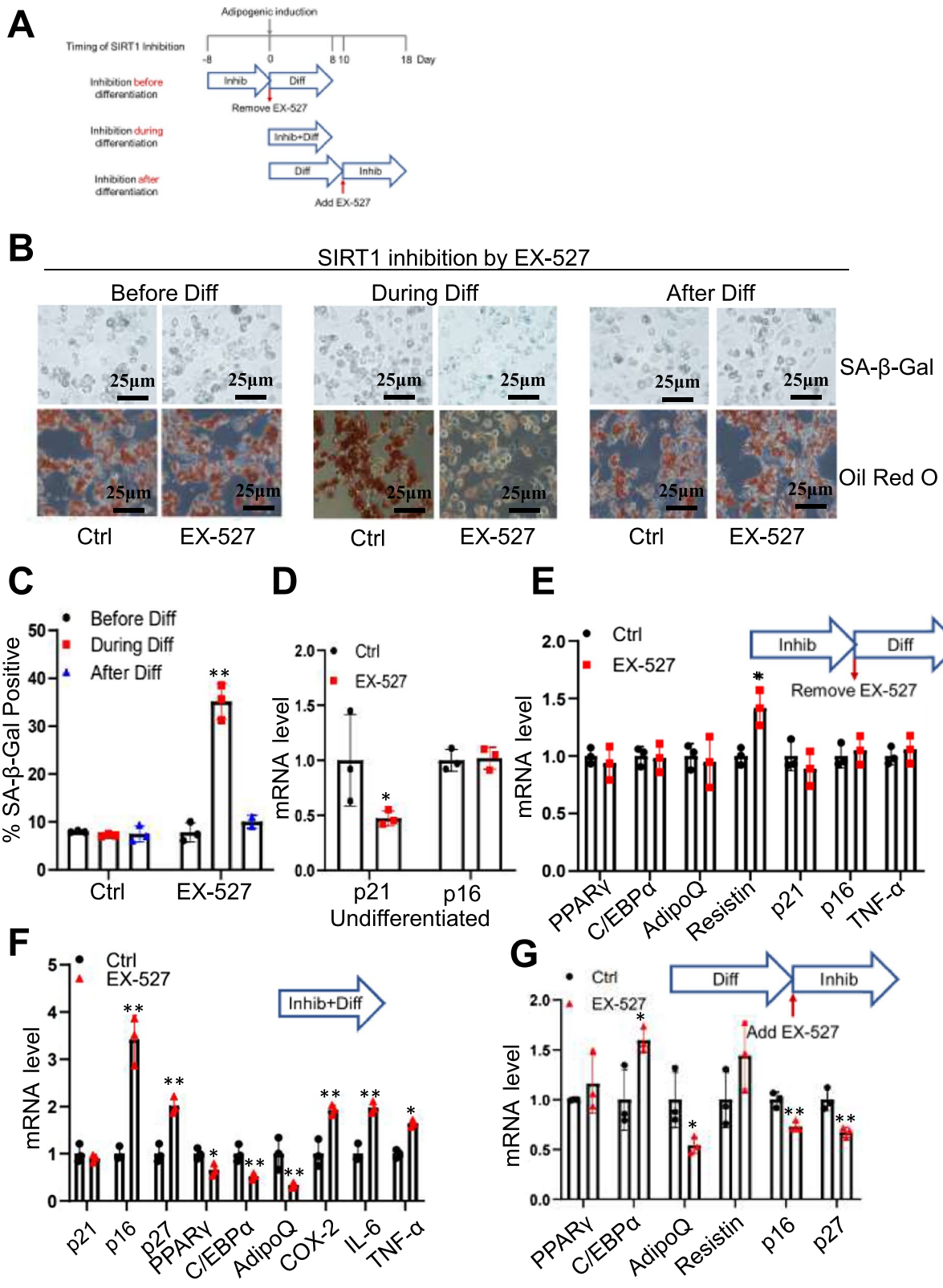
A
Adipogenic induction
Timing of SIRT1 Inhibition
-8
0
8 10
18 Day
Inhibition before differentiation
Inhib
Diff
Remove EX-527
Inhibition during differentiation
Inhib+Diff
Inhibition after differentiation
Diff
Inhib
Add EX-527
B
SIRT1 inhibition by EX-527
Before Diff
During Diff
After Diff
SA-β-Gal
Oil Red O
25μm
Ctrl
EX-527
C
Before Diff
During Diff
After Diff
% SA-β-Gal Positive
Ctrl
EX-527
D
Ctrl
EX-527
mRNA level
p21
p16
Undifferentiated
E
Ctrl
EX-527
Inhib
Diff
Remove EX-527
mRNA level
PPARγ
C/EBPα
AdipoQ
Resistin
p21
p16
TNF-α
F
Ctrl
EX-527
Inhib+Diff
mRNA level
p21
p16
p27
PPARγ
C/EBPα
AdipoQ
COX-2
IL-6
TNF-α
G
Ctrl
EX-527
Diff
Inhib
Add EX-527
mRNA level
PPARγ
C/EBPα
AdipoQ
Resistin
p16
p27

◂**Fig. 2** Adipocytes defects caused by SIRT1 activity inhibition is timing dependent. (Ctrl: control, KD: knockdown, SA-β-Gal: senescence associated β galactosidase, Inhib: inhibition, Diff: differentiation, AdipoQ: adiponectin, One-Way ANOVA test was used for multi-group statistical comparison.) (**A**) Experimental design for SIRT1 activity inhibition at different cellular stages from undifferentiated C3H10T1/2 mesenchymal stem cells to mature C3H10T1/2 adipocytes. The concentration of SIRT1 inhibitor EX-527 is 60 μM to severely impair SIRT1 activity. Cells were treated with EX-527 for 8 days, and fresh medium containing EX-527 was added every other day. The control is 0.05% DMSO. (**B**) SIRT1 activity inhibition during adipogenic differentiation decreased lipid droplet accumulation and increased SA-β-Gal activity, whereas SIRT1 activity inhibition for 8 days both before and after adipogenic differentiation did not affect lipid droplet accumulation and SA-β-Gal activity. (**C**) Quantification of SA-β-Gal activity positive cells, (Data represent mean ± SD, 3 groups of cells were counted, each group 60 cells, $^{**}p < 0.01$). (**D**) In undifferentiated cells, 8 days of EX-527 treatment did not affect the p16 mRNA level (Data represent mean ± SD, $n = 3$, $^{*}p < 0.05$). (**E**) Pre-treatment with EX-527 for 8 days following 8 days of adipogenic differentiation without EX-527 did not increase p16 mRNA compared to the control group. (Data represent mean ± SD, $n = 3$, $^{*}p < 0.05$). (**F**) Treatment with EX-527 for 8 days during adipogenic differentiation significantly increased p16 mRNA and decreased adipocyte genes mRNA (Data represent mean ± SD, $n = 3$, $^{*}p < 0.05$, $^{**}p < 0.01$). (**G**) Treatment with EX-527 in mature adipocytes for 8 days did not up-regulate p16 mRNA (Data represent mean ± SD, $n = 3$, $^{*}p < 0.05$, $^{**}p < 0.01$)

SIRT1 inhibition during adipogenic differentiation decreased the size of lipid droplets in adipocytes (Fig. S3B), which might be a phenotype of adipocyte browning. To test this possibility, we analyzed expression levels of browning markers PRDM16, UCP-1 and PGC-1α by qPCR and found that none of these browning factors showed increased expression, ruling out this scenario (Fig. S3C). Together, these results indicated that SIRT1 plays a significant role in preventing the rapid development of cellular senescence and dysfunctional adipocytes formation during adipogenic differentiation, while its activity inhibition is dispensable for the induction of rapid cellular senescence in MSCs (Fig. 2D, S2C, and S3A) and differentiated adipocytes (Fig. 2G).

Consistent phenotypes for SIRT1 impairment in human MSCs and mouse inguinal adipose tissue

Next, we investigated whether similar differentiation defects can also be observed in human umbilical cord-derived primary MSCs when SIRT1 activity was inhibited by EX-527. Indeed, we found similarly decreased lipid droplets accumulation, elevated SA-β-galactosidase activities, decreased adiponectin expression, and increased expression of senescence marker p16 compared to controls (Fig. 3A-D), confirming SIRT1's functions in supporting adipogenic differentiation and preventing cellular senescence during MSC differentiation.

To determine whether SIRT1 plays similar roles in adipogenic differentiation in vivo, we generated MSC-specific SIRT1 knockout mice (SIRT1 MSCKO) as described previously [22]. At 14 months of age, inguinal adipose tissues were collected from both the SIRT1 MSCKO mice and their wildtype littermates. We found that p16 levels were noticeably increased in SIRT1 MSCKO compared to the wild type (Fig. 3E and Fig. S9B). In contrast, heterozygous MSC-specific SIRT1 knockout mice (cre+; flox/-) exhibited no notable change in p16 expression levels in inguinal adipose tissues (Fig. S3D and Fig. S10B). These results suggest that only complete loss of SIRT1 activities in MSCs is sufficient to cause increased p16 in inguinal adipose tissues. The inguinal fat pad, but not other fat depots, in SIRT1 MSCKO mice was noticeably smaller than that of the wildtype littermates (Fig. 3F), consistent with the previous finding of significant subcutaneous adipose tissue reduction in SIRT1 MSCKO mice [22]. Strikingly, SA-β-Gal staining revealed that inguinal adipose tissues from SIRT1 MSCKO mice contained more SA-β-Gal positive cells compared to those from control wildtype mice (Fig. 3G) and there is an increase in IL-6 protein levels in the inguinal adipose tissues in SIRT1 MSCKO mice (Fig. 3H and Fig. S9C). These observations suggest that severe loss of SIRT1 in MSCs results in a significant increase in cellular senescence and a dramatic decrease of subcutaneous adipose tissues, providing in vivo evidence for our finding that SIRT1 also functions to support adipogenic differentiation in MSCs.

Inefficient expression of antioxidant enzymes is partially responsible for differentiation defects observed during SIRT1 inhibition

Increased reactive oxygen species (ROS) plays a role in promoting adipogenic differentiation in both human MSCs and mouse 3T3-L1 pre-adipocytes [30]. Interestingly, an opposite role for ROS on adipogenic differentiation has also been reported. In

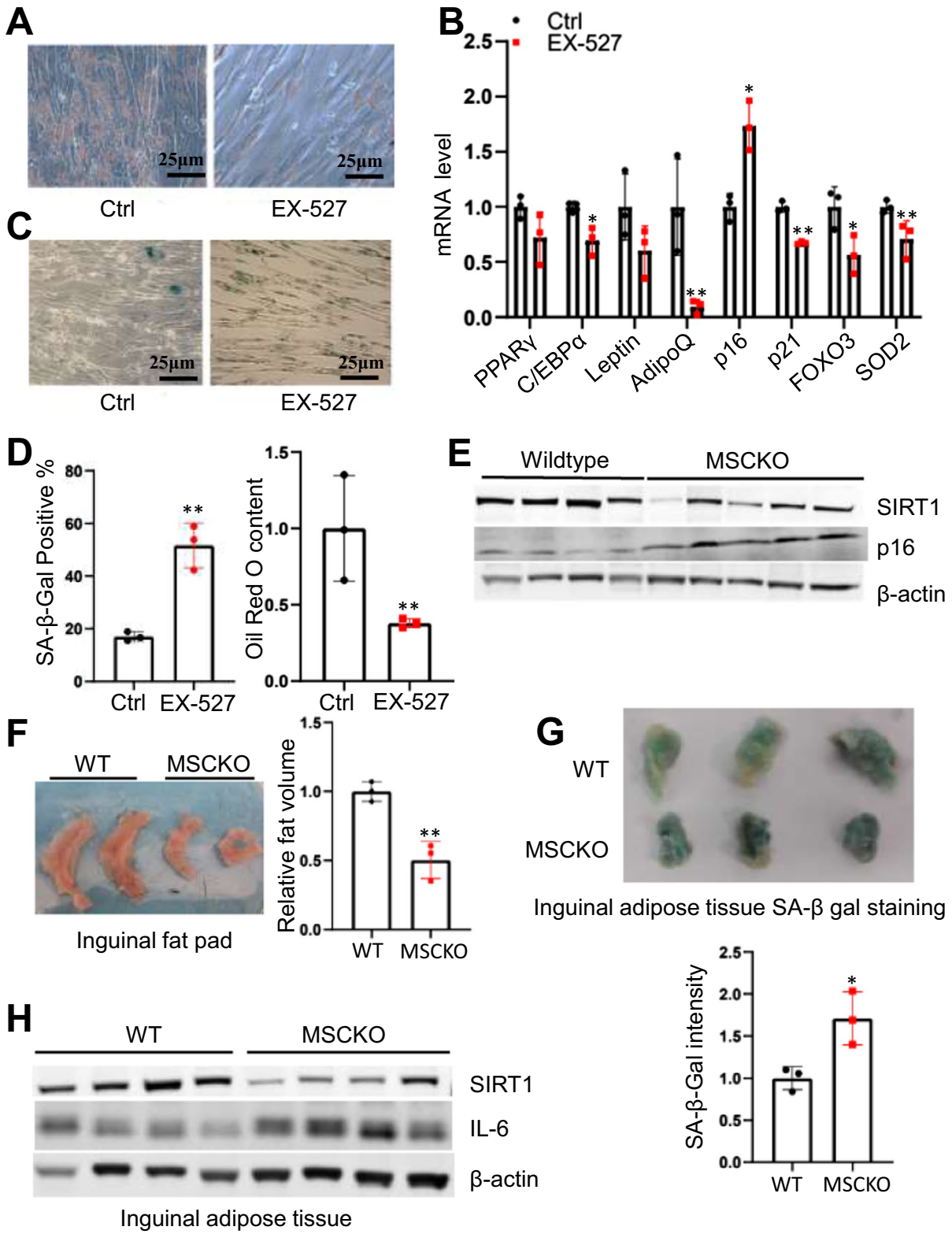
A
25μm
25μm
Ctrl
EX-527
B
Ctrl
EX-527
mRNA level
PPARγ
C/EBPα
Leptin
AdipoQ
p16
p21
FOXO3
SOD2
C
25μm
25μm
Ctrl
EX-527
D
SA-β-Gal Positive %
Ctrl
EX-527
Oil Red O content
Ctrl
EX-527
E
Wildtype
MSCKO
SIRT1
p16
β-actin
F
WT
MSCKO
Inguinal fat pad
Relative fat volume
WT
MSCKO
G
WT
MSCKO
Inguinal adipose tissue SA-β gal staining
SA-β-Gal intensity
WT
MSCKO
H
WT
MSCKO
SIRT1
IL-6
β-actin
Inguinal adipose tissue

◂**Fig. 3** Severe SIRT1 function impairment in MSCs increased cellular senescence in human cells during adipogenic differentiation as well as in mouse inguinal adipose tissue. (Ctrl: control, uMSCs: human umbilical cord mesenchymal stem cells, MSCKO: mesenchymal stem cells specific SIRT1 knockout, AdipoQ: adiponectin, WT: wild type) (**A**) and (**D**) Treatment with EX-527 in human primary uMSCs during 15 days of adipogenic differentiation decreased lipid droplet accumulation. Fresh medium containing EX-527 was added every other day. The control is 0.05% DMSO. EX-527 concentration is 60 μM. (**B**) Treatment with EX-527 in human primary uMSCs during adipogenic differentiation decreased adipocytes genes mRNA and increased p16 mRNA (Data represent mean ± SD, $n = 3$, $*p < 0.05$, $**p < 0.01$). (**C**) and (**D**) EX-527 treatment during adipogenic differentiation in human uMSCs significantly increased SA-β-Gal activity positive cells. (Data represent mean ± SD, 3 groups of cells were counted, each group 60 cells, $**p < 0.01$). (**E**) SIRT1 protein levels are lower and the p16 protein level is higher in the inguinal adipose tissue of 14 month old female SIRT1 MSCKO mice. Wild type $n = 4$, SIRT1 MSCKO $n = 5$. The genotype of wild type mice is flox/flox, cre-; the genotype of SIRT1 MSCKO mice is flox/flox, cre + . The body weight of wildtype mice: 29.3 g, 28.1 g, 31.2 g, 30.6 g; the body weight of SIRT1 MSCKO mice:26.6 g, 29.1 g, 27.6 g, 28.6 g, 29.3 g. (**F**) The inguinal fat pads of SIRT1 MSCKO mice are smaller than the inguinal fat pads of wild type mice. (**G**) The SA-β-Gal activity is higher in the inguinal adipose tissue of SIRT1 MSCKO mice ($n = 3$) compared to wild type mice ($n = 3$). (**H**) IL-6 protein level is higher in the inguinal adipose tissue of 14 months old female SIRT1 MSCKO mice. The body weight of wildtype mice: 28.8 g, 32.1 g, 30.5 g, 31.7 g; the body weight of SIRT1 MSCKO mice:27.7 g, 29.5 g, 30.6 g, 28.3 g. Note: SIRT1 levels were reduced but remained detectable due to the presence of tissues developed from other stem cells other than the MSCs. Wild type $n = 4$, SIRT1 MSCKO $n = 4$

mouse 3T3-L1 cells, H_2O_2 (0.1–0.5 mM) treatments diminished the expression of adipocytokines, such as adiponectin and the adipogenic master regulator PPARγ [31]. In mice, oxidative stress accumulates in adipose tissue during aging and inhibits adipogenesis [32]. Notably, even though ROS promotes adipogenic differentiation, the induction of antioxidant enzymes, such as superoxide dismutase 2 (SOD2) and Catalase, are critical for adipogenesis. Failure to induce their expression by FOXO1 (Forkhead box 1) knockdown leads to significantly repressed adipogenesis in human MSCs [33].

Given these observations on the importance of oxidative stress response and the implication of SIRT1 in mitigating excessive ROS by mediating oxidative stress response [34], we hypothesize that even though high levels of ROS are necessary for adipogenic differentiation, proper oxidative stress response regulated by SIRT1 antagonizing the adverse effects of ROS accumulation is critical for healthy adipogenesis. To test this hypothesis, we measured ROS levels by Dihydroethidium (DHE) staining before, during, and after adipogenic differentiation in mouse C3H10T1/2 MSCs. There were low levels of ROS in cells prior to differentiation (day -2 and day 0), followed by a progressive increase in ROS levels during adipogenic differentiation, which peaked at day 8 of the differentiation process (Fig. 4A and S8A). There was a slight but notable reduction in ROS levels at the late stage of adipogenic differentiation (days 10 and 12 after induction), compared to days 6 and 8 (Fig. 4A and S8A). The ROS level during differentiation was also detected by DCFDA staining (Fig. S10 G), the result is similar to DHE staining. The observed increases and subsequent decreases in ROS levels during adipogenic differentiation were commensurate with changes in mitochondria copy numbers (Fig. S4A). Hence, these observations indeed suggest that differentiating cells undergo high oxidative stress during adipogenic differentiation. Intriguingly, inhibition of SIRT1 by EX-527 during the adipogenic differentiation resulted in further increased ROS levels in day 8 differentiating cells compared to non-inhibited controls (Fig. 4B and S8B). Moreover, differentiating MSCs (after eight days of adipogenic induction), showed significant increases in SOD2 and Catalase expression compared to undifferentiated cells. This increase was significantly compromised in differentiating cells with EX-527 treatment (Fig. 4C). These results suggest that oxidative stress response is elevated during adipogenic differentiation to antagonize increased ROS levels, which is necessary for the process, and that inhibition of SIRT1 compromises the oxidative response resulting in excessive ROS levels that cause cellular senescence in differentiating cells. To further test this possibility, we treated MSCs with relatively high levels of H_2O_2 (300 μM) during the eight days of adipogenic differentiation and found that lipid droplets accumulation was dramatically reduced (Fig. 4E and S8C) and the cellular senescence marker p16 was significantly activated (Fig. 4F), recapitulating the effects of SIRT1 inhibition by EX-527. It is important to note that moderate levels of H_2O_2 (100 μM) had no so such detrimental effects on adipogenic differentiation (Fig. 4F). Interestingly, when the EX-527-treated cells were also incubated with the anti-oxidant NAC (1 mM) during

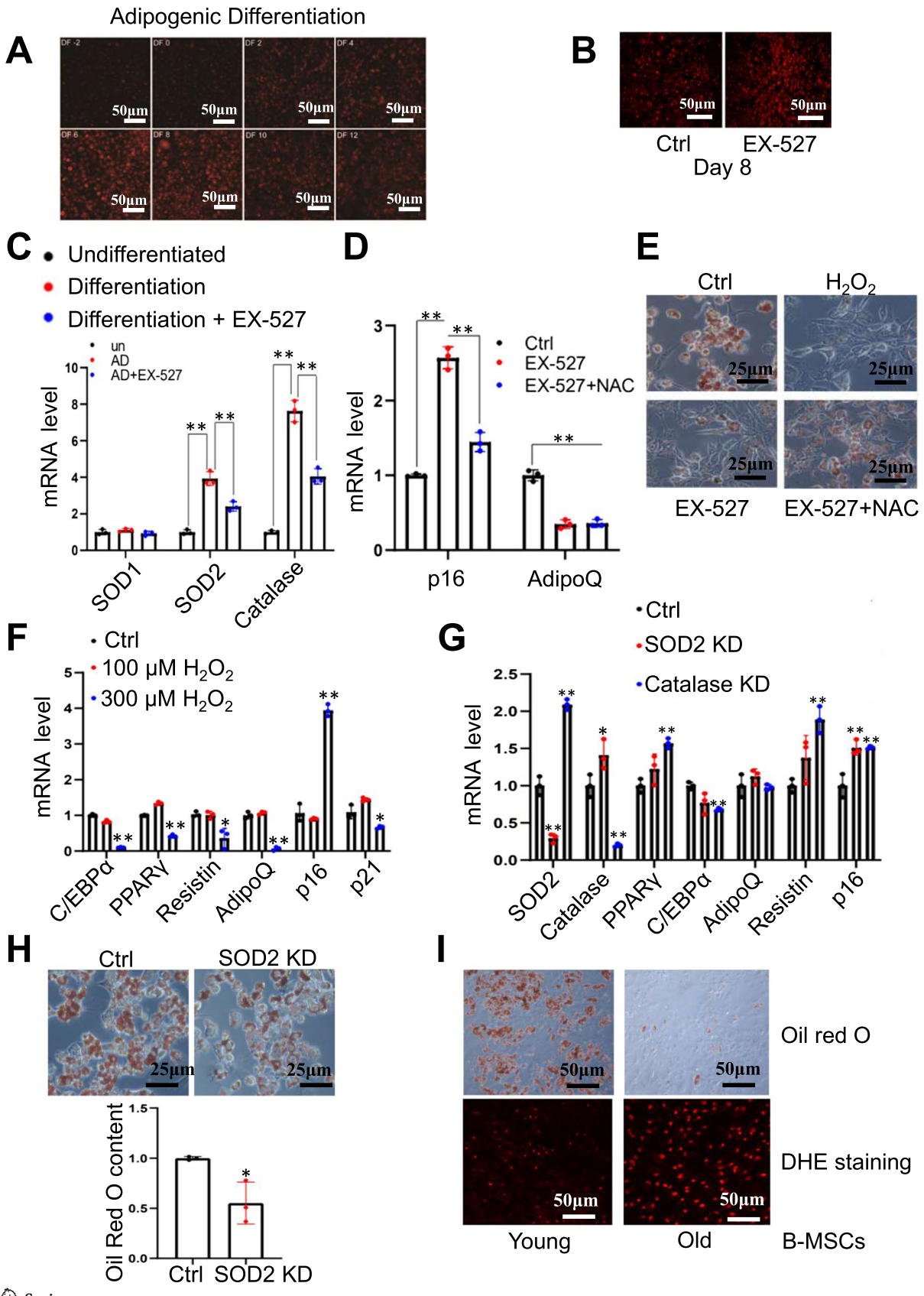
Adipogenic Differentiation
A
DF -2
DF 0
DF 2
DF 4
DF 6
DF 8
DF 10
DF 12
50μm
B
Ctrl
EX-527
Day 8
C
Undifferentiated
Differentiation
Differentiation + EX-527
un
AD
AD+EX-527
mRNA level
SOD1
SOD2
Catalase
D
Ctrl
EX-527
EX-527+NAC
mRNA level
p16
AdipoQ
E
Ctrl
H2O2
25μm
EX-527
EX-527+NAC
F
Ctrl
100 μM H2O2
300 μM H2O2
mRNA level
C/EBPα
PPARγ
Resistin
AdipoQ
p16
p21
G
Ctrl
SOD2 KD
Catalase KD
mRNA level
SOD2
Catalase
PPARγ
C/EBPα
AdipoQ
Resistin
p16
H
Ctrl
SOD2 KD
25μm
Oil Red O content
Ctrl
SOD2 KD
I
50μm
Oil red O
DHE staining
Young
Old
B-MSCs

◂**Fig. 4** Anti-oxidant enzymes contribute to decrease p16 expression during adipogenic differentiation. (Ctrl: control, DHE: Dihydroethidium, NAC: N-acetylcysteine, SOD: superoxide dismutase, KD: knockdown, AdipoQ: adiponectin, Y-B-MSCs: human primary bone marrow mesenchymal stem cells from 24 years old donor, O-B-MSCs: human primary bone marrow mesenchymal stem cells from 73 years old donor, One-Way ANOVA test was used for multi-group statistical comparison.). (**A**). ROS level is increasing during adipogenic differentiation and became decreased after adipogenic differentiation day 8 (DF: differentiation). (**B**) SIRT1 inhibition by EX-527 (60 μM) further increased ROS level upon adipogenic differentiation. (**C**) SIRT1 inhibition by EX-527 (60 μM) significantly deceased SOD2 and Catalase mRNA levels upon adipogenic differentiation (Data represent mean ± SD, $n = 3$, $*p < 0.05$, $**p < 0.01$). (**D**-**E**) Anti-oxidant NAC (1 mM) partially rescued adipogenic differentiation defects, including lipid droplets accumulation and p16 expression, caused by EX-527 (60 μM); whereas H_2O_2 (300 μM) decreased lipid droplets accumulation (Data represent mean ± SD, $n = 3$, $*p < 0.05$, $**p < 0.01$). (**F**) 300 μM but not 100 μM H_2O_2 decreased adipocyte genes expression and increased p16 mRNA expression during adipogenic differentiation (Data represent mean ± SD, $n = 3$, $*p < 0.05$, $**p < 0.01$). (**G**) SOD2 or Catalase knockdown significantly increased p16 mRNA expression during adipogenic differentiation (Data represent mean ± SD, $n = 3$, $*p < 0.05$, $**p < 0.01$). (H) SOD2 knockdown decreased lipid droplet accumulation upon adipogenic differentiation. (I) Bone marrow mesenchymal stem cells from young donor have higher adipogenic differentiation efficiency than B-MSCs from old donor. O-B-MSCs accumulated more ROS than Y-B-MSCs in response to 15 days of adipogenic induction

adipogenic differentiation, the defects in adipogenesis were substantially rescued, including restored lipid droplet accumulation as well as suppressed p16 expression (Fig. 4D-E and S8C). The anti-oxidative enzymes SOD2 and Catalase are activated by SIRT1-mediated oxidative stress response[35, 36]. To determine whether the down-regulation of these anti-oxidative enzymes contributes to adipogenic differentiation defects observed in cells inhibited for SIRT1, stable SOD2 and Catalase knockdown strains were generated by lentivirus mediated shRNA transfection in C3H10T1/2 MSCs (Fig. 4G). In undifferentiated cells, SOD2 or Catalase knockdown for eight days up-regulates some SIRT1 related anti-oxidative factors such as Nrf2, FOXO3 and SUV39H1 (Fig. S4B), indicating a cellular response to increased oxidative stress. Importantly, p16 expression was not significantly elevated under these conditions (Fig. S4B) suggesting SOD2 or Catalase knockdown alone prior to adipogenic differentiation does not cause cellular senescence. In contrast, knocking down SOD2 or Catalase during the eight days of adipogenic differentiation caused reduced lipid droplet accumulation and significantly increased p16 expression (Fig. 4G-H and S8D), recapitulating the effects of SIRT1 inhibition. Inhibiting SIRT1 activity by EX-527 (60 μM) for eight days in undifferentiated C3H10T1/2 MSCs did not decrease the expression levels of SOD2 and Catalase (Fig. S8I), suggesting that the basal expression of SOD2 and Catalase may not be dependent on SIRT1. Together, these results demonstrate that SIRT1 supports adipogenic differentiation and prevents cellular senescence in MSCs through its functions in activating cellular oxidative stress response. Impaired SIRT1 functions and weakened oxidative stress response have been associated with tissue and stem cell aging. Using human bone marrow-derived mesenchymal stem cells (B-MSCs) isolated from young (24-year old) and old (73-year old) donors, we tested the efficiency of adipogenic differentiation as well as ROS levels. After 15 days of adipogenic differentiation, old B-MSCs displayed dramatically poorer adipogenic differentiation compared to the young B-MSCs (Fig. 4I and S8E), as well as much higher ROS levels (Fig. 4I and S8E), suggesting that more increased ROS accumulation during adipogenic differentiation might be a cause for adipogenic defects in human MSCs, similar to what has been observed in mice [32]. SIRT1 protein levels and its downstream targets Suv39h1, and H3K9me3 levels in these young and old B-MSCs were shown in Fig. S10H.

Increased physical interaction between SIRT1 and FOXO3 in response to oxidative stress is one of the key cellular anti-oxidative actions [16], by which SIRT1 finetunes the activities of FOXO3 to induce cell cycle arrest and oxidative stress response, and to inhibit apoptosis [16]. FOXO3 protein levels dramatically increased during the course of adipogenic differentiation (Fig. S6A and Fig. S10C), indicating that its functions may be important for the process. In undifferentiated replicating MSCs, FOXO3 localized to the cytoplasm; when they are arrested due to contact inhibition [37], FOXO3 translocated into the nucleus (Fig. S6B). Cellular contact inhibition is important for the successful induction of adipogenic differentiation (Fig. S5A). Interestingly, one day after adipogenic induction, FOXO3 was found exclusively into the cytoplasm, suggesting that differentiating cells overcome the regulatory pathways of contact inhibition (Fig. S6C). Furthermore, FOXO3 started

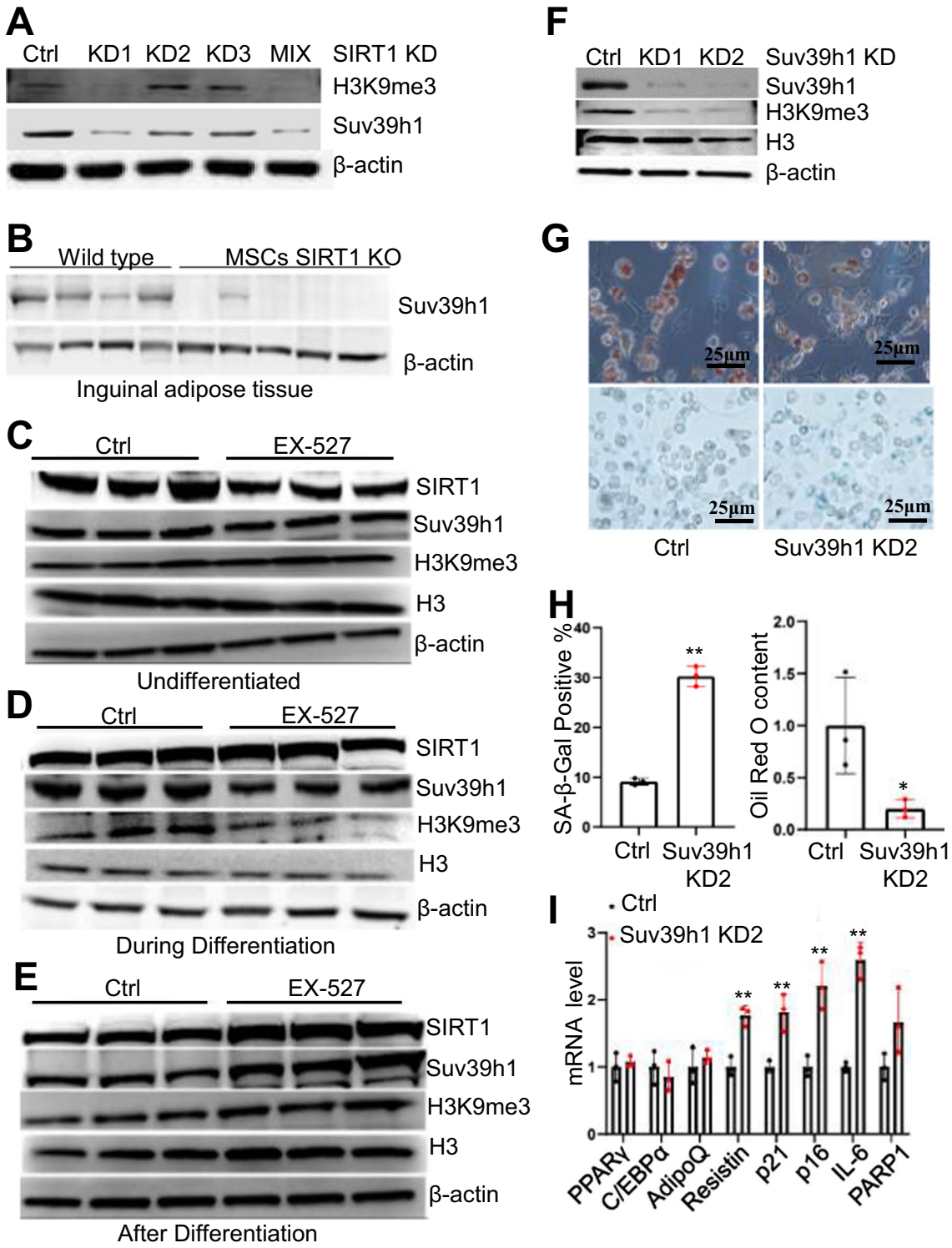

to translocate into the nucleus at day four of adipogenic differentiation and by day six FOXO3 became evenly distributed between cytoplasm and nucleus despite the higher levels of insulin in the adipogenic

◂**Fig. 5** SUV39H1-H3K9me3 pathway mediated SIRT1 severe impairment induced cellular senescence during adipogenic differentiation. EX-527 concentration 60 μM. (**A**) SIRT1 knockdown decreased SUV39H1 protein level, but only severe SIRT1 knockdown (SIRT1 KD1 and SIRT1 KD MIX) decreased H3K9me3 level. (**B**) The SUV39H1 protein level is lower in the inguinal adipose tissue of 14 months old female SIRT1 MSCKO mice. Wild type $n=4$, SIRT1 MSCKO $n=5$. (**C**) In undifferentiated mouse MSCs, 8 days of SIRT1 inhibition by EX-527 did not decrease both SUV39H1 and H3K9me3 levels. (**D**) 8 days SIRT1 inhibition by EX-527 during adipogenic differentiation decreased both SUV39H1 and H3K9me3 level. (**E**) 8 days SIRT1 inhibition by EX-527 in mature adipocytes increased both SUV39H1 and H3K9me3 level. (**F**) SUV39H1 knockdown strongly decreased the H3K9me3 level. (**G**) Severe SUV39H1 knockdown (KD2) decreased lipid droplet accumulation and increased SA-β-Gal activity. (**H**) Quantification of SA-β-Gal activity positive cells and Oil Red O staining content in Fig. 5G. (Data represent mean ± SD, 3 groups of cells were counted, each group 60 cells, $^{**}p<0.01$). (**I**) Severe SUV39H1 knockdown significantly increased p16, IL-6, and p21 mRNA but did not change adipocyte genes expression upon 8 days adipogenic induction (Data represent mean ± SD, $n=3$, $^{*}p<0.05$, $^{**}p<0.01$)

induction medium (Fig. S6C). Although inhibition of SIRT1 by EX-527 during adipogenic differentiation did not affect the nucleus translocation of FOXO3 (Fig. S6D), co-immunoprecipitation showed a weakened physical interaction between SIRT1 and FOXO3 (Fig. S6E and Fig. S10D). And this effect was not seen in undifferentiated MSCs (Fig. S6E and Fig. S10D). Consistent with the weakened SIRT1-FOXO3 interaction, acetylation of FOXO3 was also increased in response to SIRT1 inhibition during adipogenic differentiation (Fig. S6F and Fig. S10E), indicating compromised FOXO3 activities. We generated stable FOXO3 knockdown strains in C3H10T1/2 (Fig. S6G and Fig. S10E) and tested adipogenic differentiation efficiency. There was a decreased lipid accumulation in severe FOXO3 knockdown cells (Fig. S6I). Moreover, pro-inflammatory adipokines resistin and IL-6 were significantly up-regulated, whereas SOD2, adiponectin and SIRT1 were down-regulated (Fig. S6H), partially recapitulating the adipogenic differentiation defects caused by impairment of SIRT1 function during the differentiation.

Ataxia telangiectasia-mutated (ATM) kinase was knocked down to investigate if a DNA damage repair pathway is involved in the adipogenic defects (Fig. S7A) caused by SIRT1 impairment, and the results (Fig. S7B-D) showed that the DNA damage repair pathway did not contribute to adipogenic defects in response to severe inhibition or knockdown of SIRT1.

SUV3-9 expression decreases in response to SIRT1 inhibition during differentiation

SUV39H1 (Suppressor of variegation 3–9 homolog 1) is a key methyl-transferase responsible for Histone H3 lysine 9 tri-methylation (H3K9me3) and heterochromatin formation. SIRT1 activates SUV39H1 by direct deacetylation [38]. Under oxidative stress, SUV39H1 levels increase in a SIRT1 dependent manner, boosting the stability of the heterochromatin [39]. With age, SUV39H1 decreases in both HSCs [40] and MSCs [41], resulting in the loss of H3K9me3 and heterochromatin, which is a driver of aging phenotypes [41]. Hence, we tested the protein levels of SUV39H1 in stable SIRT1 knockdown C3H10T1/2 MSC strains (Fig. 1A). As predicted, SUV39H1 levels were decreased in all SIRT1 knockdown strains compared to the control knockdown. Moreover, reduced H3K9me3 levels were also detected in cells with severe SIRT1 knockdown (Fig. 5A and Fig. S9D), commensurate with the adipogenic differentiation defect phenotype (Fig. 1B and 1D). Therefore, to get a better picture of how SIRT1 dysfunction may affect SUV39H1 and H3K9me3 levels, we performed experiments similar to those shown in Fig. 2A and compared SUV39H1 and H3K9me3 levels at different time points in cells treated with EX-527 before, during, and after adipogenic differentiation. The SIRT1 interacting protein SUV39H1 level is very low in the inguinal adipose tissues from SIRT1 MSCKO mice (Fig. 5B and Fig. S9E). In undifferentiated C3H10T1/2 MSCs, there was no obvious change in either SUV39H1 or H3K9me3 after SIRT1 was inhibited for eight days (Fig. 5C and S8F). Interestingly, as predicted, when SIRT1 was inhibited during eight-day adipogenic differentiation, both SUV39H1 and H3K9me3 levels were significantly decreased, even though no detectable changes to SIRT1 levels were found (Fig. 5D and S8G). In differentiated adipocytes, SIRT1 inhibition caused increases in SIRT1, SUV39H1, and H3K9me3 levels, consistent with normal oxidative stress response (Fig. 5E and S8H). These results suggest that SIRT1 activity is specifically required during adipogenic

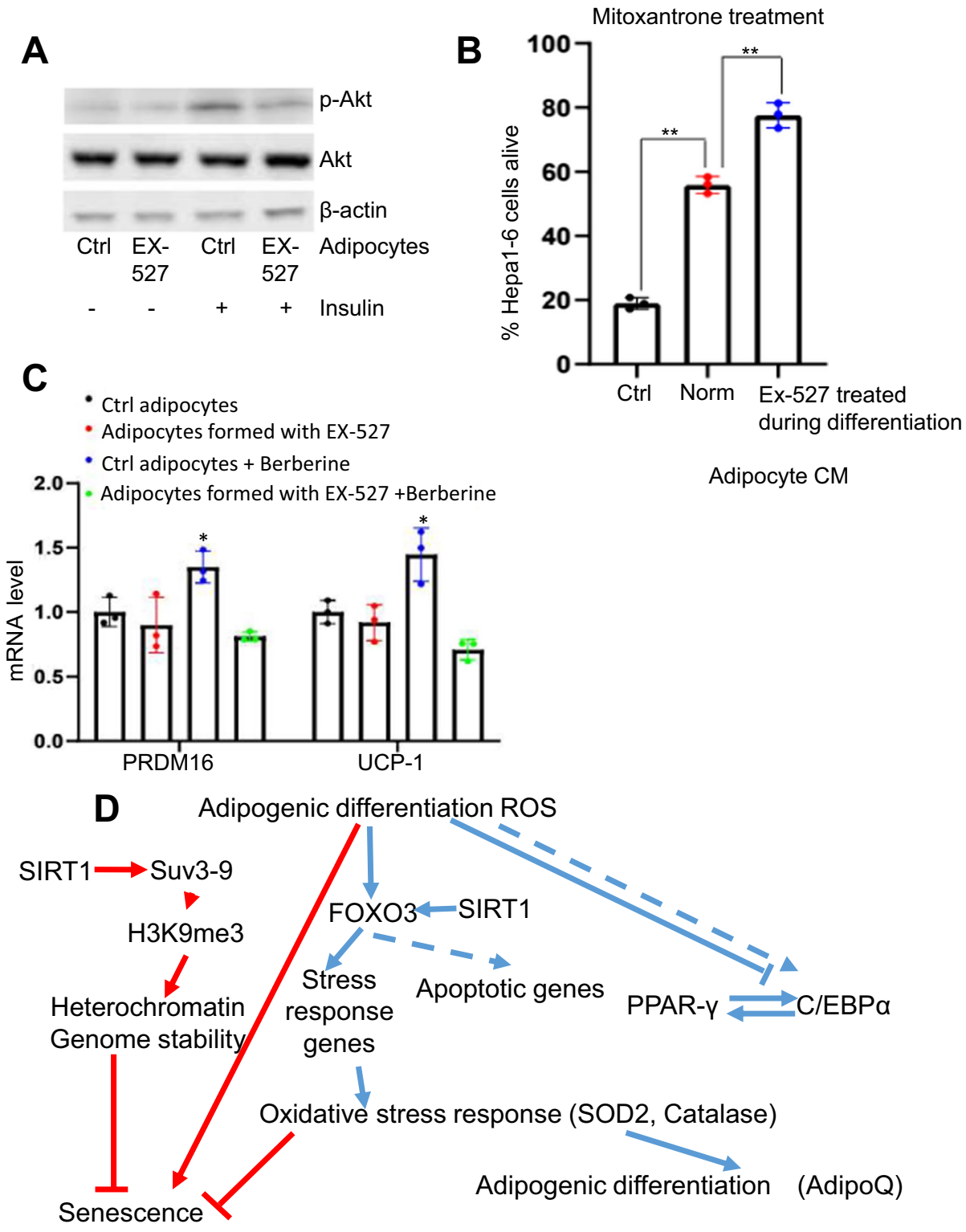
A
p-Akt
Akt
β-actin
Ctrl
EX-527
Ctrl
EX-527
Adipocytes
-
-
+
+
Insulin
B
Mitoxantrone treatment
% Hepa1-6 cells alive
100
80
60
40
20
0
**
**
Ctrl
Norm
Ex-527 treated during differentiation
Adipocyte CM
C
Ctrl adipocytes
Adipocytes formed with EX-527
Ctrl adipocytes + Berberine
Adipocytes formed with EX-527 +Berberine
mRNA level
2.0
1.5
1.0
0.5
0.0
*
*
PRDM16
UCP-1
D
Adipogenic differentiation ROS
SIRT1
Suv3-9
H3K9me3
Heterochromatin
Genome stability
FOXO3
SIRT1
Stress response genes
Apoptotic genes
PPAR-γ
C/EBPα
Oxidative stress response (SOD2, Catalase)
Adipogenic differentiation
(AdipoQ)
Senescence

◂**Fig. 6** Senescent adipocytes produced by SIRT1 inhibition during their differentiation are dysfunctional. The one-way ANOVA test was used for multi-group statistical comparison. (**A**) Senescent adipocytes caused by SIRT1 inhibition during differentiation have lower insulin sensitivity than normally differentiated adipocytes. Adipocytes were well maintained in high glucose DMEM medium with 5% FBS for 48 h then were treated with 500 nM insulin for 10 min. (**B**) Senescent adipocyte conditioned medium conferred liver cancer cells higher chemoresistance than the conditioned medium from normal adipocytes. Mouse liver cancer Hepa1-6 cells were pre-treated with adipocyte conditioned medium for 48 h, then were treated with fresh adipocyte conditioned medium containing chemotherapy reagent mitoxantrone (1.5 μM) for another 48 h (Data represent mean ± SD, 3 groups cells of each treatment were counted, $^{**}p < 0.01$). (**C**) Berberine is not able to induce senescent adipocyte browning (Data represent mean ± SD, $n = 3$, $^{*}p < 0.05$). (**D**) Severe impairment of SIRT1 function in MSCs may cause adipogenic differentiation defects through SUV39H1 and FOXO3 pathways. The SIRT1-SUV39H1-H3K9me3 pathway which contributes to increased cellular senescence during adipogenic differentiation is highlighted in red color

differentiation in order to maintain proper levels of SUV39H1 and H3K9me3, as part of the oxidative response at the chromatin level.

We then wonder whether reduced SUV39H1 activities and decreased H3K9me3 levels may also be responsible for the adipogenic defects caused by SIRT1 inhibition. To test this possibility, we generated two stable knockdown lines for SUV39H1 in C3H10T1/2 MSCs (Fig. 5F and Fig. S9F) and carried out adipogenic differentiation for the strain with higher knockdown efficiency. In undifferentiated cells, SUV39H1 knockdown for eight days did not cause proliferation defects or cellular senescence (data not shown). After eight days of adipogenic differentiation, SUV39H1 knockdown cells accumulated fewer lipid droplets than the control cells (Fig. 5G-H). The number of SA-β-Gal positive cells is significantly increased (Fig. 5G-H). Cellular senescence genes p16 and p21, as well as the pro-inflammatory adipokines resistin and IL-6, were all significantly up-regulated in SUV39H1 knockdown cells (Fig. 5I). These results suggest that SUV39H1 knockdown partially recapitulates the adipogenic defects observed in SIRT1 knockdown or inhibition cells, and loss of H3K9me3 plays a pivotal role in mediating increased cellular senescence in MSCs without SIRT1 function during adipogenic differentiation.

Adipocytes resulted from SIRT1 inhibition during differentiation are dysfunctional

We found that SIRT1 inhibition during adipogenic differentiation caused significant down-regulation of autophagy genes (Fig. S5B), which indicates a cellular malfunction. Thus, we used this model to further characterize the adipocyte functions in the senescent adipocytes, which remain largely unknown.

Insulin-AKT signaling is an important pathway that regulates blood glucose homeostasis, lipid metabolism, growth, and aging. Adipose tissue is one of the major target organs for insulin. Pro-inflammatory adipokines are thought to be important mediators of insulin resistance [42]. Based on the fact that higher blood glucose level was observed in MSCs specific SIRT1 knockout mice [22], and senescent adipocytes from SIRT1 inhibition during adipogenic differentiation (Fig. 2B and F) have higher TNF-α and IL-6 expression (Fig. 2F), we investigated whether Akt phosphorylation level is changed in response to insulin in senescent adipocytes. Normally differentiated C3H10T1/2 and adipocytes formed by SIRT1 inhibition during differentiation, two days after EX-527 removal, were incubated in normal high glucose DMEM medium with 5% FBS for 2 days, then these adipocytes were treated with insulin (500 nM) for 10 min. As shown in Fig. 6A, without insulin treatment, phosphorylation levels of AKT kinase are very low in both groups. Upon insulin treatment, phosphorylation levels of AKT kinase are increased in both groups of adipocytes, yet the phosphorylation level of AKT kinase is lower in the SIRT1 inhibition induced adipocytes formed with EX-527 compared to normal adipocytes (Fig. 6A and Fig. S9G), indicating the decreased insulin effect in these adipocytes formed with EX-527.

A well-characterized hallmark of senescent cells is the Senescence Associated Secretory Phenotype (SASP), which facilitates cancer cells' survival in response to chemotherapy drug treatment [43, 44]. To test whether adipocytes produced by SIRT1 inhibition can secrete adipokines with similar effects to SASP, adipocyte conditioned media were collected by incubating normal and adipocytes formed with EX-527 with 5% FBS DMEM media for 48 h. Mouse liver cancer cells Hepa1-6 were pre-incubated in the adipocyte conditioned media for 48 h, followed by the chemotherapy drug mitoxantrone

(1.5 μM) in conditioned media for another 48 h. Fresh 5% FBS DMEM was used as the untreated control. We found that while mitoxantrone killed most of the Hepa1-6 cells in the control group, adipocyte conditioned media significantly increased the survival of Hepa1-6 cancer cells with the adipocyte conditioned media from the senescent adipocytes formed with EX-527 having more dramatic effects (Fig. 6B and S5D). The IL-6 concentration in conditioned media was measured by ELISA, the results are shown in supplementary Fig. S10F.

Epithelial-to-mesenchymal transition (EMT) is a key molecular mechanism conferring chemoresistance in cancer cells [45, 46]. To test whether EMT was involved in the chemoresistance induced by adipokines, EMT gene (Prrx-1, Twist1, Snai-1, Snai-2, and Zeb1) expression levels were measured by qPCR in Hepa1-6 cells treated with adipocyte conditioned media. We found that both normal and senescent adipocyte conditioned media significantly increased certain EMT gene expression, including Prrx-1, which was induced by 10 folds (Fig. S5C). Notably, the adipocyte conditioned media from adipocytes formed with EX-527 resulted in a stronger induction of Snai-2 than the normal adipocyte conditioned media did, suggesting the increased chemoresistance caused by adipocytes formed with EX-527 is likely mediated by further activated EMT (Fig. S5C). Adipocyte conditioned media contain much higher IL-6 levels than the control group (Fig. S10F), which might be responsive to increased EMT in Hepa1-6 cells.

Cellular senescence, especially the MAPK p38-p16 pathway, impedes cold induced adipocytes browning during adipogenic differentiation[47]. We treated differentiated C3H10T1/2 adipocytes with berberine to induce browning [48]. Browning genes (PRDM-16 and UCP-1) were activated by berberine in control C3H10T1/2 adipocytes but failed to be activated in senescent adipocytes caused by SIRT1 inhibition (Fig. 6C), suggesting significant defects in browning of these adipocytes.

Taken together, these results demonstrate that adipocytes resulted from SIRT1 inhibition during adipogenic differentiation are dysfunctional. These defects are manifested by their higher insulin resistance, loss of browning transdifferentiation, and increased efficiency in promoting chemoresistance in liver cancer cells.

Discussion

Pro-longevity factor SIRT1 is a multi-functional protein, and its roles in the suppression of adipogenic differentiation has been demonstrated by several studies both in vitro and in vivo. For instance, SIRT1 overexpression mice have significantly less white adipose tissue than the control mice [49]. A study in humans also demonstrated that in human visceral adipose stem cells, SIRT1 and SIRT2 expression levels are negatively associated with the adipogenic differentiation capacity of these stem cells and SIRT1 overexpression resulted in the inhibition of adipocyte differentiation [50]. It was reported that complete loss of SIRT1 (SIRT1-/-) decreases adipogenic differentiation of mouse ESC to mature adipocytes [51]. This result proved that although SIRT1 has traditionally been considered as an adipogenic suppressor, it does play a role in supporting adipogenic differentiation. Our results (Fig. 1A-D) might explain the seemingly contradictory dual roles of SIRT1 in adipogenic differentiation may be dependent on its expression levels. When SIRT1 is overexpressed or moderately knocked down [50], its function as an adipogenic suppressor can be observed; when SIRT1 is completely knocked out [51], which is also shown in our CRISPR/cas9 experiments (Fig. S1A-E), its function as an adipogenic supporter/safeguard can be observed.

Lipodystrophy refers to a group of rare diseases characterized by the generalized or partial absence of adipose tissue. Not only obesity but also lipodystrophy is usually accompanied by insulin resistance syndrome, implying dysfunctional adipocytes in both adipose tissue diseases. An extreme example of lipodystrophy is the fat-specific PPARγ-knockout mice, which exhibited much less adipose tissue and extreme insulin resistance [52]. Similar to lipodystrophy syndromes, aging is associated with the loss of subcutaneous adipose tissues in the elderly, affects the distribution of limb fat and trunk fat, and increases insulin resistance [53]. In both young and old MSC-specific SIRT1 knockout mice, there is a significant loss of subcutaneous adipose tissue with smaller adipocytes and these mice have metabolic syndrome [22]. These are features of lipodystrophy. The contradictory effects of SIRT1 on adipose tissue formation suggest that SIRT1 must also play a role in supporting healthy adipogenic differentiation in addition to

its adipogenic suppression function. Accumulation of senescent cells in adipose tissues during aging is a potent inducer of lipodystrophy, and clearance of senescent cells increases adipogenesis [54], prevents lipodystrophy, and increases insulin sensitivity in old mice [55]. This current study highlighted a previously unnoticed role of SIRT1 in preventing senescence during adipogenic differentiation. Our results suggest that increased cellular senescence in subcutaneous adipose tissue of MSC-specific SIRT1 knockout mice (Fig. 3E and 3G) might be the underlying cause of lipodystrophy features observed in these mice [22].

Given that SIRT1 activities, as well as NAD^+ concentrations, decrease with age, the Nampt-SIRT1 pathway has been considered one of the important mechanisms that control the balance of adipogenic differentiation and osteogenic differentiation in MSCs [56]. A general paradigm of SIRT1-regulated differentiation balance is that the high level/activity of SIRT1 facilitates osteogenic differentiation and the low level/activity of SIRT1 promotes adipogenic differentiation [57]. Our findings add new insights to this paradigm by demonstrating that adipogenic differentiation efficiency is not increased when SIRT1 level is too low and dysfunctional adipocytes will form (Fig. 6A-C) as a result of adipogenic differentiation when SIRT1 is defective. Hence, SIRT1 at least plays three different roles in adipogenesis: First, SIRT1 is a negative regulator of adipogenic differentiation as demonstrated by many previous studies; second, our present study indicates that SIRT1 is a safeguard for adipogenic differentiation to prevent cell senescence by maintaining cellular anti-oxidative stress response; third, SIRT1 is an important positive regulator of white adipocytes browning [58].

SIRT1 is an enzyme with many substrates. How SIRT1's activities toward different substrates are regulated remains poorly understood. On one hand, among these SIRT1 targets, some of them might be very sensitive to SIRT1 activity and moderate SIRT1 function impairment is enough to affect their functions; whereas, others might be less sensitive to SIRT1 function and their activities are only affected when SIRT1 function was severely impaired. On the other hand, SIRT1 has preferred targets especially when SIRT1 activity is limited. For example, under oxidative stress, SIRT1 leaves its original locations in heterochromatin and translocates to DNA double strand break sites to facilitate the DNA repair process [59]. In this study, results from cells with different SIRT1 protein dosages (Fig. 1A) showed that only severe SIRT1 knockdown decreased H3K9me3 levels (Fig. 5A), suggesting that either SUV39H1 function is less sensitive to SIRT1 levels or SUV39H1 is a not preferred target of SIRT1. Specifically regards to the adipogenic differentiation process, moderate loss of SIRT1 function may increase PPARγ functions [19] and decrease Wnt pathway activities [21] to promote adipogenic differentiation; whereas severe loss of SIRT1 function affects pathways such as SUV39H1-H3K9me3 [40, 41], leading to lipodystrophy-like phenotypes [22]. Therefore, moderate and severe SIRT1 knockdown have opposite effects on adipogenic differentiation (Fig. 1B). In general, at least a certain degree of SIRT1 is required to support healthy adipogenic differentiation by raising cellular anti-oxidative response, including maintaining H3K9me3 heterochromatin level (Fig. 5D) and upregulating anti-oxidative genes (Fig. 4C), upon increased ROS level during adipogenic differentiation. SIRT1's interacting targets such as Suv39h1 and Foxo3 may coordinately work with SIRT1 to maintain cellular oxidative stress response. When SIRT1 is severely impaired or completely knocked out during adipogenic differentiation, dysfunctional adipocytes would be formed, as indicated by less lipid droplet accumulation, increased senescence, reduced insulin sensitivity, loss of browning capacity, and secretions promoting cancer survival. We conclude that SIRT1 plays an essential role in preventing senescent cell formation during adipogenic differentiation by promoting cellular oxidative stress response and severe impairment of SIRT1 or complete loss of SIRT1 during adipogenic differentiation caused senescent and dysfunctional adipocyte formation. The molecular pathways for SIRT1 functions in both suppression of adipogenic differentiation and support of healthy adipocyte formation are summarized in Fig. 6D.

Acknowledgements This work was supported by Ted Nash Long Life Foundation grant award and CPRIT Scholar award R1306 to WD.

Author Contributions Conceptualization, AY and WD; Data curation, AY, RY; Formal analysis, AY and WD; Funding acquisition, WD; Investigation, AY, DJ, RY, CG and HL; Methodology, AY, DJ, RY, HL, CG and WD; Project administration, AY and WD; Resources, AY and WD; Supervision, WD; Validation, AY and WD; Writing- Original Draft, AY, and WD; Writing- review & editing, AY, RY, HL, and WD.

Data Availability Data sharing is not applicable to this article as no new sequencing data were created or analyzed in this study.

Declarations

Conflict of interest The authors declare that there is no conflicting interest in this study.

References

1. Rosen ED, Spiegelman BM. Adipocytes as regulators of energy balance and glucose homeostasis. Nature. 2006;444(7121):847–53.
2. Argmann C, et al. Ppargamma2 is a key driver of longevity in the mouse. PLoS Genet. 2009;5(12):e1000752.
3. Despres JP, Lemieux I. Abdominal obesity and metabolic syndrome. Nature. 2006;444(7121):881–7.
4. Fiorenza CG, Chou SH, Mantzoros CS. Lipodystrophy: pathophysiology and advances in treatment. Nat Rev Endocrinol. 2011;7(3):137–50.
5. Matsuzawa Y. Adiponectin: a key player in obesity related disorders. Curr Pharm Des. 2010;16(17):1896–901.
6. Ohashi K, et al. Role of anti-inflammatory adipokines in obesity-related diseases. Trends Endocrinol Metab. 2014;25(7):348–55.
7. Newsholme P, de Bittencourt Jr., PI. The fat cell senescence hypothesis: a mechanism responsible for abrogating the resolution of inflammation in chronic disease. Curr Opin Clin Nutr Metab Care. 2014;17(4):295-305.
8. Chen YW, et al. Ablation of XP-V gene causes adipose tissue senescence and metabolic abnormalities. Proc Natl Acad Sci U S A. 2015;112(33):E4556–64.
9. Campisi J, Robert L. Cell senescence: role in aging and age-related diseases. Interdiscip Top Gerontol. 2014;39:45–61.
10. Baker DJ, et al. Naturally occurring p16(Ink4a)-positive cells shorten healthy lifespan. Nature. 2016;530(7589):184–9.
11. Chang J, et al. Clearance of senescent cells by ABT263 rejuvenates aged hematopoietic stem cells in mice. Nat Med. 2016;22(1):78–83.
12. Vicencio JM, et al. Senescence, apoptosis or autophagy? When a damaged cell must decide its path–a mini-review. Gerontology. 2008;54(2):92–9.
13. Jurk D, et al. Postmitotic neurons develop a p21-dependent senescence-like phenotype driven by a DNA damage response. Aging Cell. 2012;11(6):996–1004.
14. Tan FC, et al. Are there roles for brain cell senescence in aging and neurodegenerative disorders? Biogerontology. 2014;15(6):643–60.
15. Xiong ZM, et al. An inhibitory role of progerin in the gene induction network of adipocyte differentiation from iPS cells. Aging (Albany NY). 2013;5(4):288–303.
16. Brunet A, et al. Stress-dependent regulation of FOXO transcription factors by the SIRT1 deacetylase. Science. 2004;303(5666):2011–5.
17. Langley E, et al. Human SIR2 deacetylates p53 and antagonizes PML/p53-induced cellular senescence. EMBO J. 2002;21(10):2383–96.
18. Yeung F, et al. Modulation of NF-kappaB-dependent transcription and cell survival by the SIRT1 deacetylase. EMBO J. 2004;23(12):2369–80.
19. Picard F, et al. Sirt1 promotes fat mobilization in white adipocytes by repressing PPAR-gamma. Nature. 2004;429(6993):771–6.
20. Zhou Y, et al. SIRT1 inhibits adipogenesis and promotes myogenic differentiation in C3H10T1/2 pluripotent cells by regulating Wnt signaling. Cell Biosci. 2015;5:61.
21. Zhou Y, et al. SIRT1 suppresses adipogenesis by activating Wnt/beta-catenin signaling in vivo and in vitro. Oncotarget. 2016;7(47):77707–20.
22. Simic P, et al. SIRT1 regulates differentiation of mesenchymal stem cells by deacetylating beta-catenin. EMBO Mol Med. 2013;5(3):430–40.
23. Yoon DS, et al. SIRT1 directly regulates SOX2 to maintain self-renewal and multipotency in bone marrow-derived mesenchymal stem cells. Stem Cells. 2014;32(12):3219–31.
24. Sanjana NE, Shalem O, Zhang F. Improved vectors and genome-wide libraries for CRISPR screening. Nat Methods. 2014;11(8):783–4.
25. Imperatore F, et al. SIRT1 regulates macrophage self-renewal. EMBO J. 2017;36(16):2353–72.
26. Yu A, et al. Resistin impairs SIRT1 function and induces senescence-associated phenotype in hepatocytes. Mol Cell Endocrinol. 2013;377(1–2):23–32.
27. Zhou L, et al. Resistin reduces mitochondria and induces hepatic steatosis in mice by the protein kinase C/protein kinase G/p65/PPAR gamma coactivator 1 alpha pathway. Hepatology. 2013;57(4):1384–93.
28. Zhou L, et al. Conditioned medium obtained from in vitro differentiated adipocytes and resistin induce insulin resistance in human hepatocytes. FEBS Lett. 2007;581(22):4303–8.
29. Deutsch MJ, et al. Digital image analysis approach for lipid droplet size quantitation of Oil Red O-stained cultured cells. Anal Biochem. 2014;445:87–9.
30. Atashi F, Modarressi A, Pepper MS. The role of reactive oxygen species in mesenchymal stem cell adipogenic and osteogenic differentiation: a review. Stem Cells Dev. 2015;24(10):1150–63.
31. Furukawa S, et al. Increased oxidative stress in obesity and its impact on metabolic syndrome. J Clin Invest. 2004;114(12):1752–61.
32. Findeisen HM, et al. Oxidative stress accumulates in adipose tissue during aging and inhibits adipogenesis. PLoS One. 2011;6(4):e18532.
33. Higuchi M, et al. Differentiation of human adipose-derived stem cells into fat involves reactive oxygen species and Forkhead box O1 mediated upregulation of antioxidant enzymes. Stem Cells Dev. 2013;22(6):878–88.
34. Olmos Y, et al. SirT1 regulation of antioxidant genes is dependent on the formation of a FoxO3a/PGC-1alpha complex. Antioxid Redox Signal. 2013;19(13):1507–21.
35. Guan XH, et al. CD38 Deficiency Protects the Heart from Ischemia/Reperfusion Injury through Activating

SIRT1/FOXOs-Mediated Antioxidative Stress Pathway. Oxid Med Cell Longev. 2016;2016:7410257.
36. Pardo PS, et al. Induction of Sirt1 by mechanical stretch of skeletal muscle through the early response factor EGR1 triggers an antioxidative response. J Biol Chem. 2011;286(4):2559–66.
37. Leontieva OV, Demidenko ZN, Blagosklonny MV. Contact inhibition and high cell density deactivate the mammalian target of rapamycin pathway, thus suppressing the senescence program. Proc Natl Acad Sci U S A. 2014;111(24):8832–7.
38. Vaquero A, et al. SIRT1 regulates the histone methyltransferase SUV39H1 during heterochromatin formation. Nature. 2007;450(7168):440–4.
39. Bosch-Presegue L, et al. Stabilization of Suv39H1 by SirT1 is part of oxidative stress response and ensures genome protection. Mol Cell. 2011;42(2):210–23.
40. Djeghloul D, et al. Age-Associated Decrease of the Histone Methyltransferase SUV39H1 in HSC Perturbs Heterochromatin and B Lymphoid Differentiation. Stem Cell Reports. 2016;6(6):970–84.
41 Zhang W, et al. Aging stem cells. A Werner syndrome stem cell model unveils heterochromatin alterations as a driver of human aging. Science. 2015;348(6239):1160–3.
42. Kwon H, Pessin JE. Adipokines mediate inflammation and insulin resistance. Front Endocrinol (Lausanne). 2013;4:71.
43. Demaria M, et al. Cellular Senescence Promotes Adverse Effects of Chemotherapy and Cancer Relapse. Cancer Discov. 2017;7(2):165–76.
44. Laberge RM, et al. MTOR regulates the pro-tumorigenic senescence-associated secretory phenotype by promoting IL1A translation. Nat Cell Biol. 2015;17(8):1049–61.
45. Fischer KR, et al. Epithelial-to-mesenchymal transition is not required for lung metastasis but contributes to chemoresistance. Nature. 2015;527(7579):472–6.
46. Zheng X, et al. Epithelial-to-mesenchymal transition is dispensable for metastasis but induces chemoresistance in pancreatic cancer. Nature. 2015;527(7579):525–30.
47. Berry DC, et al. Cellular Aging Contributes to Failure of Cold-Induced Beige Adipocyte Formation in Old Mice and Humans. Cell Metab. 2017;25(1):166–81.
48. Zhang Z, et al. Berberine activates thermogenesis in white and brown adipose tissue. Nat Commun. 2014;5:5493.
49. Bordone L, et al. SIRT1 transgenic mice show phenotypes resembling calorie restriction. Aging Cell. 2007;6(6):759–67.
50. Perrini S, et al. Reduced SIRT1 and SIRT2 expression promotes adipogenesis of human visceral adipose stem cells and associates with accumulation of visceral fat in human obesity. Int J Obes (Lond). 2020;44(2):307–19.
51. Jung YJ, et al. SIRT1 induces the adipogenic differentiation of mouse embryonic stem cells by regulating RA-induced RAR expression via NCOR1 acetylation. Stem Cell Res. 2020;44:101771.
52. Wang F, et al. Lipoatrophy and severe metabolic disturbance in mice with fat-specific deletion of PPARgamma. Proc Natl Acad Sci U S A. 2013;110(46):18656–61.
53. Gavi S, et al. Limb fat to trunk fat ratio in elderly persons is a strong determinant of insulin resistance and adiponectin levels. J Gerontol A Biol Sci Med Sci. 2007;62(9):997–1001.
54. Palmer AK, et al. Targeting senescent cells alleviates obesity-induced metabolic dysfunction. Aging Cell. 2019;18(3):e12950.
55. Xu M, et al. Targeting senescent cells enhances adipogenesis and metabolic function in old age. Elife. 2015;4:e12997.
56. Li Y, et al. Nicotinamide phosphoribosyltransferase (Nampt) affects the lineage fate determination of mesenchymal stem cells: a possible cause for reduced osteogenesis and increased adipogenesis in older individuals. J Bone Miner Res. 2011;26(11):2656–64.
57. Chen H, et al. Role of SIRT1 and AMPK in mesenchymal stem cells differentiation. Ageing Res Rev. 2014;13:55–64.
58. Qiang L, et al. Brown remodeling of white adipose tissue by SirT1-dependent deacetylation of Ppargamma. Cell. 2012;150(3):620–32.
59. Oberdoerffer P, et al. SIRT1 redistribution on chromatin promotes genomic stability but alters gene expression during aging. Cell. 2008;135(5):907–18.